Journal of
PERIODONTAL RESEARCH

J Periodont Res 2013; 48: 373–385

JOURNAL OF PERIODONTAL RESEARCH
doi:10.1111/jre.12017

Expression profiling of microRNAs in RAW264.7 cells treated with a combination of tumor necrosis factor alpha and RANKL during osteoclast differentiation

T. Kagiya[1], S. Nakamura[2]
[1]Division of Functional Morphology, Department of Anatomy, Iwate Medical University, Iwate, Japan and [2]Division of Maxillofacial Diagnostic and Surgical Sciences, Department of Oral and Maxillofacial Oncology, Kyushu University Graduate School of Dental Science, Fukuoka, Japan

Kagiya T, Nakamura S. Expression profiling of microRNAs in RAW264.7 cells treated with a combination of tumor necrosis factor alpha and RANKL during osteoclast differentiation. J Periodont Res 2013; 48: 373–385. © 2012 John Wiley & Sons A/S. Published by John Wiley & Sons Ltd

Background and Objective: Tumor necrosis factor alpha (TNF-α), a cytokine involved in the pathogenesis of periodontal disease, induces osteoclast differentiation and indirectly promotes alveolar bone resorption. We investigated TNF-α-regulated osteoclast differentiation, focusing on microRNAs. MicroRNAs are small, noncoding RNAs that are involved in various biological processes, including cellular differentiation, proliferation and apoptosis. Aside from miR-21, miR-155 and miR-223, the identities of the microRNAs that play roles in osteoclast differentiation are unknown. Notably, no previous studies have reported the expression profiling of microRNAs during TNF-α-regulated osteoclast differentiation.

Material and Methods: We used microarrays to screen the levels of expression of mature microRNAs in RAW264.7 cells treated with a combination of TNF-α and RANKL, or RANKL alone for 0, 24 or 82 h during osteoclast formation. We validated the results of the microarray analyses through quantitative RT-PCR analyses of representative microRNAs in RAW264.7 cells and murine bone marrow macrophages.

Results: During osteoclast formation, the expression of 44 mature microRNAs differed by more than twofold between untreated cells and cells treated with a combination of TNF-α and RANKL, and the expression of 52 mature microRNAs differed upon RANKL treatment. According to quantitative RT-PCR analyses, miR-378 was upregulated and miR-223 was downregulated during osteoclast formation. Furthermore, miR-21, miR-29b, miR-146a, miR-155 and miR-210 were highly expressed during osteoclast differentiation in TNF-α/RANKL-treated cells compared with RANKL-treated cells.

Conclusions: These results suggest that miR-223 and miR-378 may play important roles in osteoclastogenesis, and that miR-21, miR-29b, miR-146a, miR-155 and miR-210 are involved in TNF-α-regulated osteoclast differentiation.

Tadayoshi Kagiya, DDS, Division of Functional Morphology, Department of Anatomy, Iwate Medical University, 2-1-1 Nishitokuta, Yahaba-cho, Iwate, 028-3694, Japan
Tel: +81 19 651 5111
Fax: +81 19 908 8010
e-mail: tkagiya@iwate-med.ac.jp

Key words: microarray; microRNA; osteoclast dierentiation; tumor necrosis factor alpha

Accepted for publication September 1, 2012

The amount of bone in the body, including alveolar bone, is determined by the balance between bone formation and bone resorption (1). Osteoblasts are the only cells that play a role in bone formation, and osteoclasts are the only cells involved in bone resorption. Bone metabolism is maintained by strictly regulated bone remodeling (1, 2), and an imbalance of this regulation can result in numerous diseases. For example, alveolar bone loss in periodontal disease is caused by excessive bone resorption (3).

Periodontal disease is a chronic bacterial infection of tooth-supporting structures that results in the destruction of alveolar bone (4). Consistent with their essential role in bone remodeling, osteoclasts are central to this bone destruction. Osteoclasts are TRAP-positive, multinucleated giant cells that are derived from hematopoietic stem cells (2, 5, 6). Many of the cytokines involved in osteoclastogenesis have been identified. RANKL, which is expressed in osteoblasts, T cells and stromal cells, is essential for the induction of osteoclast differentiation (2, 3, 7), and tumor necrosis factor alpha (TNF-α) induces osteoclast differentiation in the presence of RANKL (8). TNF-α, a member of the TNF ligand superfamily, is secreted by many cell types, including periodontal ligament fibroblasts, gingival fibroblasts, osteoblasts, T cells and monocytes/macrophages (8–10). TNF-α is present at high levels in both gingival crevicular fluid and periodontal tissues of diseased sites, and is involved in the pathogenesis of periodontitis (11–13).

MicroRNAs (miRNAs) are small, endogenous, noncoding RNAs of approximately 22 nucleotides. More than 1150 and 1920 miRNAs have been identified in mice and humans, respectively (miRBase database, http://www.mirbase.org/). Although the biological functions of most miRNAs are not yet fully understood, they are known to participate in the regulation of cellular differentiation, proliferation, apoptosis and cancer development (1, 14–19). Transcription of miRNA genes yields noncoding transcripts, which are subsequently processed through sequential digestion by the RNase III enzymes Drosha and Dicer. The resulting single-stranded mature miRNAs are finally incorporated into an RNA-induced silencing complex that contains argonaute family proteins. These argonaute proteins recruit miRNAs specific for target mRNAs (1), and the RNA-induced silencing complex inhibits the translation of the target mRNAs and/or degrades the target mRNAs (1, 19). Thus, miRNAs are involved in the post-transcriptional regulation of mRNA function.

Recent studies have suggested that miRNAs play critical roles in periodontitis (20–22). The miRNAs expressed in periodontitis gingiva, including let-7a, let-7f, miR-19a, miR-20a, miR-30e, miR-130a, miR-142-3p and miR-301a, are upregulated by more than two- to 10-fold compared with expression in healthy gingiva (20–22). As comorbidities, obesity and periodontitis are associated with significant local upregulation of several miRNA species that share inflammatory and metabolic mRNA targets (20). Polymicrobial infection with periodontal pathogens has been shown specifically to enhance miR-146a expression in ApoE-deficient mice during experimental periodontal disease (23). Despite accumulating evidence that miRNAs are essential in the development of periodontitis, their roles in alveolar bone resorption are largely unknown. The only miRNAs that have been reported as important regulators of osteoclast differentiation are miR-21, miR-155 and miR-223. RANKL-induced c-Fos upregulates miR-21, which downregulates the expression of programmed cell death 4, a negative regulator of osteoclastogenesis (24–27). The overexpression of miR-155 blocks osteoclast differentiation by repressing microphthalmia-associated transcription factor and PU.1, which are crucial transcription factors for osteoclast differentiation (25–28). As a key factor in osteoclast differentiation, miR-223 regulates nuclear factor I-A and macrophage colony-stimulating factor (M-CSF) receptor levels (1, 25–27, 29, 30). Notably, no reports have described the expression profiling of miRNAs during the differentiation of osteoclasts treated with TNF-α. Hypothesizing that many miRNAs participate in TNF-α-regulated osteoclast differentiation, we performed miRNA expression profiling using microarrays.

Material and methods

RAW 264.7 cell culture

Murine RAW264.7 macrophages, obtained from the American Type Culture Collection (ATCC) (Manassas, VA, USA), were seeded at a cell density of 20,000 cells/cm^2 and cultured in Dulbecco's modified Eagle's medium (Invitrogen, Fredrick, MD, USA) supplemented with 10% fetal bovine serum (Moregate Biotech, Bulimba, Qld, Australia). After incubation for 24 h, the growth medium was replaced with alpha-minimum essential medium (α-MEM; Invitrogen), and the cells were incubated without antibiotics for an additional 82 h at 37°C in a humidified atmosphere containing 5% CO_2, in the presence of recombinant human soluble RANKL (PeproTech EC, London, UK) and/or recombinant murine TNF-α (PeproTech, Rocky Hill, NJ, USA).

Bone marrow macrophage culture

All animal experiments were reviewed and approved by the Animal Use and Care Committee of Iwate Medical University (registration number: 23-029). Five-week-old male ddY mice were purchased from Japan SLC, Inc. (Hamamatsu, Japan). The mice were killed, and their femurs and tibias were removed and dissected free of adherent soft tissue. The ends of the bones were cut, and a 25-gauge needle was used to inject α-MEM into one end of the bone and slowly flush the marrow cavity. The marrow cells were collected, and the red blood cells were removed by treatment with phosphate-buffered saline (pH 7.2) containing 10 mM Tris and 0.83% NH_4Cl. After two washes with α-MEM, the cells were seeded at a cell density of 200,000 cells/cm^2 and then cultured in α-MEM containing 10% fetal bovine serum and 10 ng/mL

of recombinant mouse M-CSF (R&D Systems, Inc., Minneapolis, MN, USA), without antibiotics. After 2 d, the medium was changed, and the cells were cultured in the presence of M-CSF (10 ng/mL), TNF-α (50 ng/mL) and RANKL (20 ng/mL), or in the presence of M-CSF (10 ng/mL) and RANKL (100 ng/mL), for up to 82 h.

Microarray analysis

Using a mirVana™ miRNA isolation kit (Ambion, Austin, TX, USA), total RNA (including miRNA) was harvested from RAW264.7 cells that had been treated with TNF-α/RANKL or RANKL alone for 0, 24 or 82 h. RNA quality was assessed by determining the absorption of the RNA at 230 nm (A_{230}), 260 nm (A_{260}) and 280 nm (A_{280}), and showing that the A_{260}/A_{280} was > 1.8 and that the A_{260}/A_{230} was > 2.0. Lack of RNA degradation was further confirmed using an Agilent 2100 Bioanalyzer (Agilent Technologies, Santa Clara, CA, USA). After assessing RNA quality, labeled total RNA samples (100 ng each) were prepared according to the Agilent miRNA Microarray System protocol using a miRNA Complete Labeling and Hyb Kit (Agilent Technologies). According to the manufacturer's protocol, no specific molecule is appropriate for normalization of Agilent miRNA microarray data, and the adjustment of total RNA (100 ng) was used as a substitute for sample normalization. The samples were then hybridized to Agilent mouse miRNA microarrays (version 2) (666 miRNAs based on miRBase database release 12.0). The data were analyzed using Agilent Feature Extraction software and GeneSpring GX software (Agilent Technologies).

Quantitative RT-PCR analysis of mRNA and miRNA expression

Using a mirVana™ miRNA isolation kit, total RNA was harvested from RAW264.7 cells that had been treated with TNF-α/RANKL or RANKL for 0, 12, 24, 48 or 82 h. Total RNA was harvested from bone marrow macrophages (BMMs), treated with TNF-α/RANKL/M-CSF or RANKL/M-CSF for 0, 24 or 82 h, also using the mirVana™ miRNA isolation kit. To measure mRNA expression, the RNA was reverse-transcribed using ReverTra Ace (Toyobo, Osaka, Japan) and random primers (Toyobo). The resulting complementary DNAs were then amplified using SYBR Premix EX Taq II (Takara Bio, Otsu, Japan) with gene-specific primers (Takara Bio) (Table S1). Target gene expression in each sample was normalized to the glyceraldehyde-3-phosphate dehydrogenase signal. The $2^{-\Delta\Delta C_t}$ method was used to calculate relative mRNA expression levels.

To evaluate miRNA expression, the RNA was reverse-transcribed using a TaqMan MicroRNA Reverse Transcription Kit (Applied Biosystems, Foster City, CA, USA) with miRNA-specific primers (Applied Biosystems). The expression of mature miRNAs was analyzed using appropriate TaqMan miRNA assays (Applied Biosystems). Quantification was performed using snoRNA 202 as an endogenous control (31, 32). The $2^{-\Delta\Delta C_t}$ method

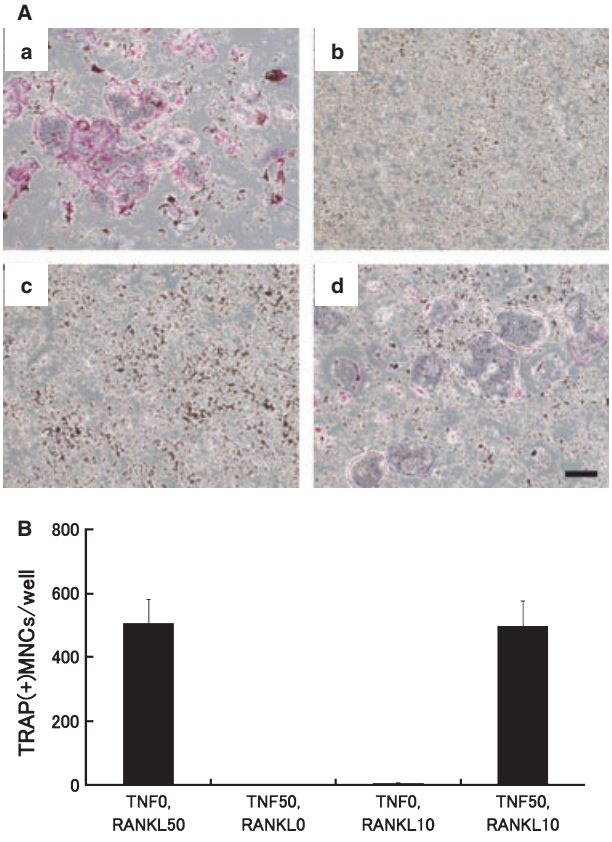

Fig. 1. Effect of tumor necrosis factor alpha (TNF-α) on osteoclastogenesis. RAW264.7 cells were seeded on 24-well plates and incubated for 82 h with RANKL (0, 10 or 50 ng/mL) and/or TNF-α (0 or 50 ng/mL). (A) Representative microscopic images of RAW264.7 cells stimulated with RANKL and/or TNF-α and stained for TRAP. Osteoclasts did not form in the presence of TNF-α (50 ng/mL) alone. a, RANKL (50 ng/mL) alone; b, TNF-α (50 ng/mL) alone; c, RANKL (10 ng/mL) alone; d, TNF-α (50 ng/mL) and RANKL (10 ng/mL). Bar, 100 μm. (B) Number of TRAP-positive multinucleated cells (MNCs) per well. Osteoclasts did not form in the presence of TNF-α alone. Few osteoclasts formed in the presence of RANKL (10 ng/mL) alone. Similar numbers of osteoclasts formed from RAW264.7 cells treated with TNF-α (50 ng/mL) plus RANKL (10 ng/mL) and from cells treated with RANKL (50 ng/mL) alone. Data are presented as mean ± standard deviation of three wells. RANKL0, 0 ng/mL of RANKL; RANKL10, 10 ng/mL of RANKL; TNF0, 0 ng/mL of TNF-α; TNF50, 50 ng/mL of TNF-α.

was used to calculate relative miRNA expression levels.

TRAP staining

At the end of the culture period, the cells were fixed with formalin/acetone/citrate (10%/65%/25%) for 1 min at room temperature, and were stained for TRAP using an acid phosphatase assay kit (Sigma-Aldrich, St Louis, MO, USA), according to the manufacturer's protocol. The numbers of TRAP-positive multinucleated cells ($\geq$ 3 nuclei) were quantified as a measure of osteoclast formation.

Statistical analysis

Data are presented as mean ± standard deviation. For multiple-group comparisons, one-way analysis of variance (ANOVA) was performed. For two independent groups, unpaired two-tailed Student's *t*-tests were used, assuming unequal variance, to identify statistically significant differences (*$p < 0.05$; **$p < 0.01$).

Results

RAW264.7 cells treated with TNF-α alone did not differentiate into osteoclasts

To investigate whether TNF-α induces osteoclast differentiation, we treated RAW264.7 cells with recombinant murine TNF-α. Osteoclasts did not form in the presence of TNF-α alone (Fig. 1). We therefore treated RAW264.7 cells with a combination of TNF-α and RANKL. Although the osteoclasts that formed from cells treated with a combination of TNF-α (50 ng/mL) and RANKL (10 ng/mL) were smaller than those that formed from cells treated with RANKL (50 ng/mL) alone (Fig. 1A), the number of osteoclasts that formed did not differ significantly between the two treatments (Fig. 1B). Therefore, in subsequent experiments we used cells treated with a combination of TNF-α (50 ng/mL) and RANKL (10 ng/mL).

RAW264.7 cells differentiate into osteoclasts after stimulation with TNF-α/RANKL for 82 h

To test the properties of the RAW264.7 cells used, cells were cultured in the presence of TNF-α and RANKL, defined as TNF-α/RANKL, and the expression of osteoclast-related genes was evaluated by quantitative RT-PCR (qRT-PCR). According to the results of the qRT-PCR analysis, the expressions of nuclear factor kappa-light-chain-enhancer of activated B cells (*Nfκb*) and nuclear factor of activated T-cells, cytoplasmic, calcineurin-dependent 1 (*Nfatc1*) (the latter of which is a master regulator of osteoclast differentiation) were transiently upregulated, peaking at 24 and 48 h, respectively (Fig. 2A, B). Moreover, the osteoclast-specific genes calcitonin receptor (*Ctr*) and *Trap* were strongly expressed after treatment with TNF-α/RANKL for 82 h (Fig. 2C, D). Based on these observations, we concluded that mature osteoclasts formed after stim-

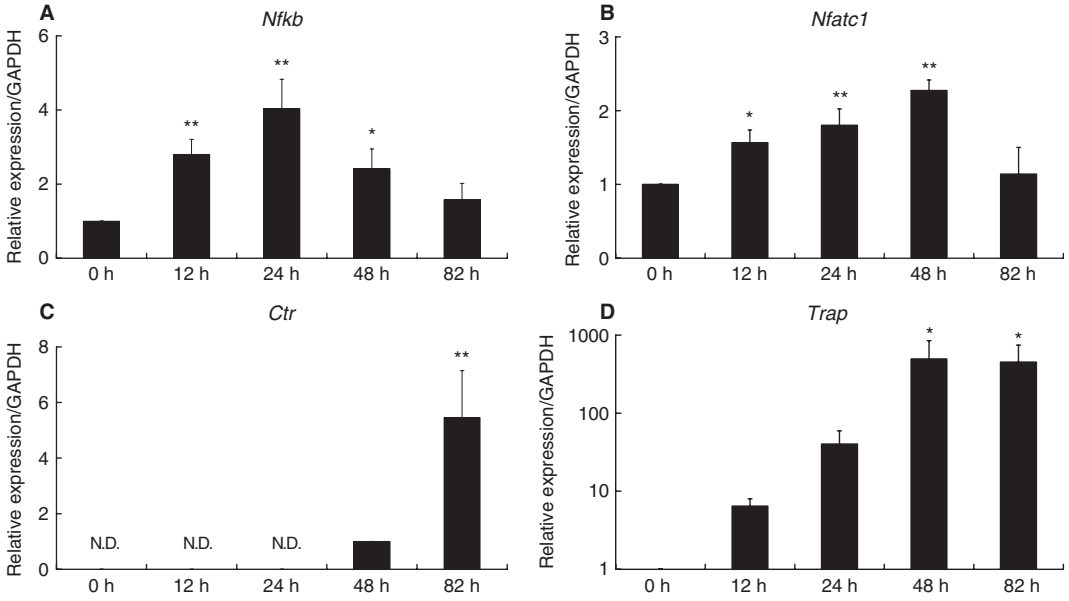

Fig. 2. Osteoclast gene expression in RAW264.7 cells after stimulation with tumor necrosis factor alpha (TNF-α)/RANKL. RAW264.7 cells were cultured in the presence of TNF-α (50 ng/mL) and RANKL (10 ng/mL). Relative expression of the osteoclast genes nuclear factor kappa-light-chain-enhancer of activated B cells (*Nfκb*) (A), nuclear factor of activated T-cells, cytoplasmic, calcineurin-dependent 1 (*Nfatc1*) (B), calcitonin receptor (*Ctr*) (C) and *Trap* (D) in RAW264.7 cells treated with TNF-α/RANKL for 0, 12, 24, 48 or 82 h, as measured by quantitative RT-PCR. Values are relative to 1 at 0 h (before stimulation) for each mRNA (A, B, D), and mRNA at 48 h (C). Target gene expression in each sample was normalized to the glyceraldehyde-3-phosphate dehydrogenase (GAPDH) signal. The experiments were performed independently three times. Data are presented as mean ± standard deviation. N.D., not detected. One-way analysis of variance was performed. *, $p < 0.05$ vs. 0 h. **, $p < 0.01$ vs. 0 h.

ulation with TNF-α/RANKL for 82 h.

The expression of 44 mature miRNAs differed by more than twofold between untreated and TNF-α-/RANKL-treated RAW264.7 cells

To screen the expression profiles of miRNAs in RAW264.7 cells treated with a combination of TNF-α and RANKL during osteoclast differentiation, we performed a microarray analysis. Figure 3 shows a heat map displaying miRNAs whose expression was altered by more than twofold in TNF-α/RANKL-treated RAW264.7 cells. Table S2 shows signal intensities for these miRNAs. The expression levels of 44 mature miRNAs varied by more than twofold, and most were upregulated in TNF-α/RANKL-treated cells. The expression levels of miR-29b, miR-125a-3p, miR-378, miR-483, miR-680 and miR-721 were upregulated, whereas miR-223 and miR-342-3p showed time-dependent downregulation in TNF-α/RANKL-treated cells. The expression levels of miR-26a, miR-199a-3p, miR-210, miR-671-5p, miR-689 and miR-1224 were decreased at 24 h, but increased at 82 h, in TNF-α/RANKL-treated cells.

qRT-PCR analysis to validate microarray miRNA expression data in TNF-α/RANKL-treated RAW264.7 cells

To confirm the results of our microarray experiments, representative miRNAs were analyzed using qRT-PCR. The expression of miR-210 was upregulated 10.4-fold in TNF-α/RANKL-stimulated cells (Fig. 4A). Similarly to miR-210, the expression of miR-378 increased 5.9-fold (Fig. 4B). miR-1224 expression also increased, peaking 48 h after stimulation with TNF-α/RANKL (4.2-fold upregulation) (Fig. 4C). In contrast, the expression of miR-223 and miR-342-3p declined in a time-dependent manner (to 0.35-fold and 0.32-fold, respectively) in response to stimulation with TNF-α/RANKL (Fig. 4D, E). In the case of miR-483, baseline expression was relatively low and no clear correlation was observed between the microarray and the qRT-PCR data (data not shown).

The expression of miR-155 has been reported to be upregulated in activated macrophages treated with TNF-α (33). It has also been reported that c-Fos induces miR-21 during osteoclast differentiation (24, 25) and that nuclear factor kappa-light-chain-enhancer of activated B cells (NF-κB) induces miR-21 in macrophages (34). Therefore, although the expression of miR-155 and that of miR-21 did not differ by more than twofold between untreated and TNF-α-/RANKL-treated cells in our microarray experiments, their expression levels were analyzed by qRT-PCR. In our study, miR-155 expression showed a 1.5-fold transient increase at 12 h after treatment with TNF-α/RANKL, but this had decreased to 0.8-fold at 82 h (Fig. 4F). The expression of miR-21 was increased 3.2-fold at 82 h after TNF-α/RANKL treatment (Fig. 4G).

To confirm the results obtained in RAW264.7 cells, we examined the miRNA expression levels in BMMs (Figure S1). The expression levels of miR-210, miR-378 and miR-1224 were upregulated 22-fold (Figure S1A), 6.4-fold (Figure S1B) and 3.1-fold (Figure S1C), respectively, in TNF-α/RANKL/M-CSF-stimulated BMMs. The expression of miR-155 showed a marked 32-fold increase (Figure S1F), and miR-21 expression was increased 4.7-fold (Figure S1G). As in RAW264.7 cells, miR-223 expression was decreased to 0.4-fold (Figure S1D); however, instead of decreasing, miR-342-3p expression increased 2.9-

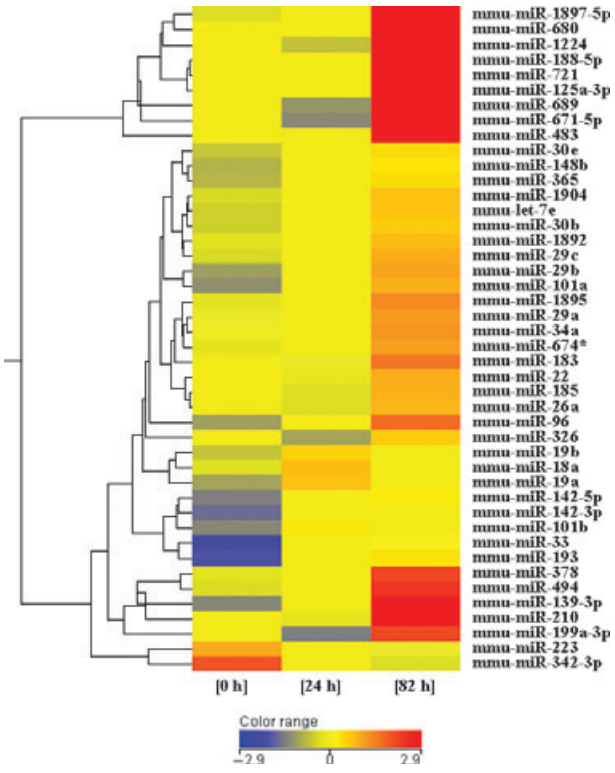

Fig. 3. MicroRNA (miRNA) expression profiles in tumor necrosis factor alpha (TNF-α)/RANKL-stimulated RAW264.7 cells. The heat map shows the results of hierarchical cluster analysis of miRNA microarray data (fold change > 2) from RAW264.7 cells stimulated with TNF-α (50 ng/mL) and RANKL (10 ng/mL) for 0, 24 or 82 h. Red, upregulation; blue, downregulation; yellow, median of the three points (0, 24 and 82 h). The miRNAs for which the signal intensities at 0, 24 and 82 h were all weak (< 20) were excluded from the map. This experiment was performed once.

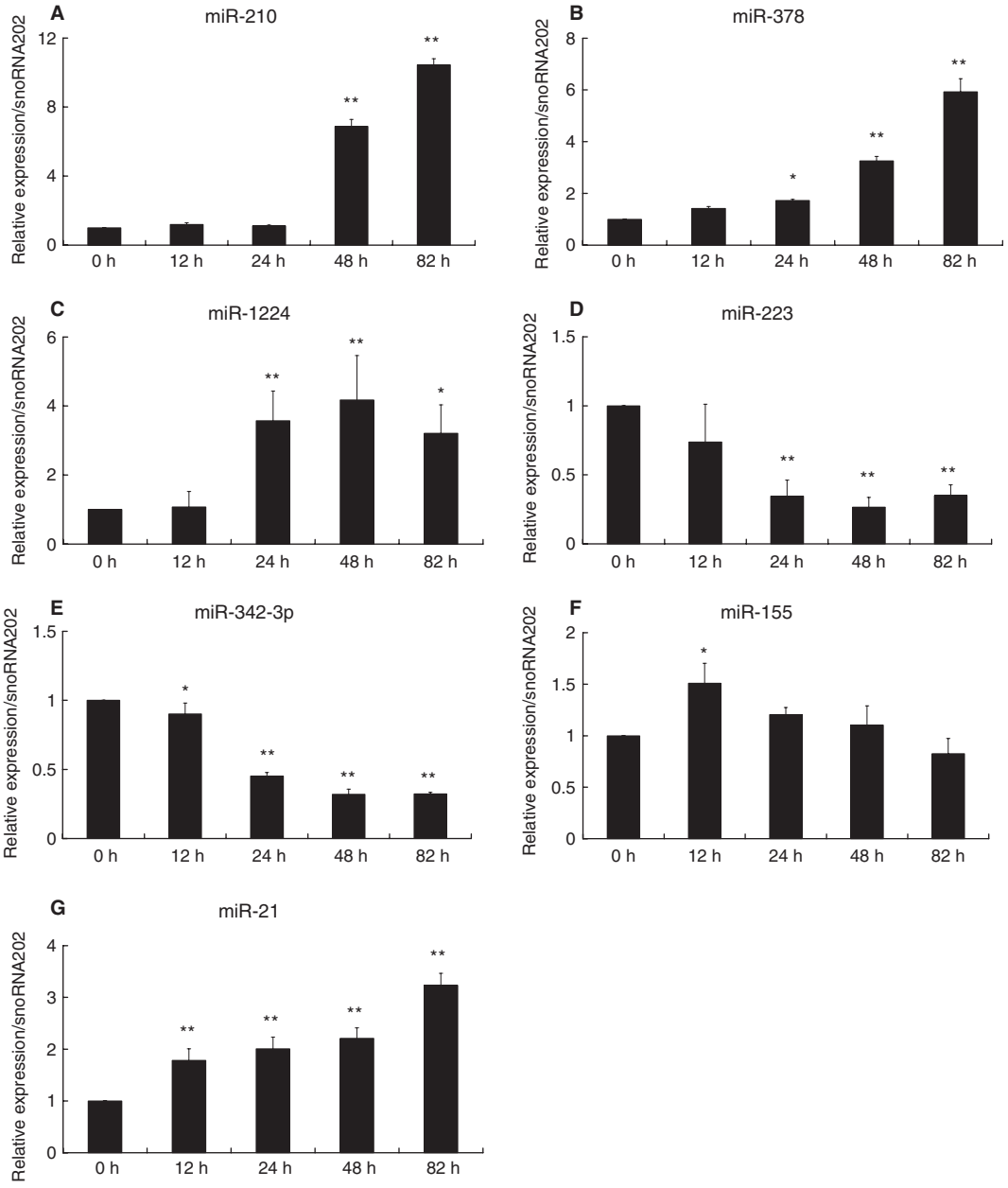

Fig. 4. Quantitative RT-PCR (qRT-PCR) validation of microRNA (miRNA) microarray data in tumor necrosis factor alpha (TNF-α)/RANKL-treated RAW264.7 cells. RAW264.7 cells were cultured in the presence of TNF-α (50 ng/mL) and RANKL (10 ng/mL) for 0, 12, 24, 48 or 82 h, and were then analyzed by qRT-PCR. The levels of expression of miR-210 (A), miR-378 (B), miR-1224 (C), miR-223 (D), miR-342-3p (E), miR-155 (F) and miR-21 (G) are shown. Values are relative to 1 at 0 h (before stimulation) for each miRNA. Quantification was performed using snoRNA 202 as an endogenous control. The experiments were performed independently three times. Data are presented as mean ± standard deviation. One-way analysis of variance was performed. *, $p < 0.05$ vs. 0 h. **, $p < 0.01$ vs. 0 h.

fold in TNF-α/RANKL/M-CSF-treated BMMs (Figure S1E).

Thus, with the exception of miR-342-3p, the changes in miRNA expression, determined by qRT-PCR and microarray analyses, were similar between TNF-α/RANKL-treated RAW264.7 cells and TNF-α/RANKL/M-CSF-treated BMMs.

Expression of 52 mature miRNAs varied by more than twofold between untreated and RANKL-treated RAW264.7 cells

To further explore changes in miRNA expression linked to osteoclast differentiation, we treated RAW264.7 cells with RANKL alone. Figure 5 shows a heat map displaying the miRNAs whose expression levels were altered by more than twofold in RANKL-treated RAW264.7 cells. Table S3 shows the signal intensities for these miRNAs. The expression of 52 mature miRNAs varied by more than twofold between untreated and RANKL-treated cells. RANKL treatment caused the

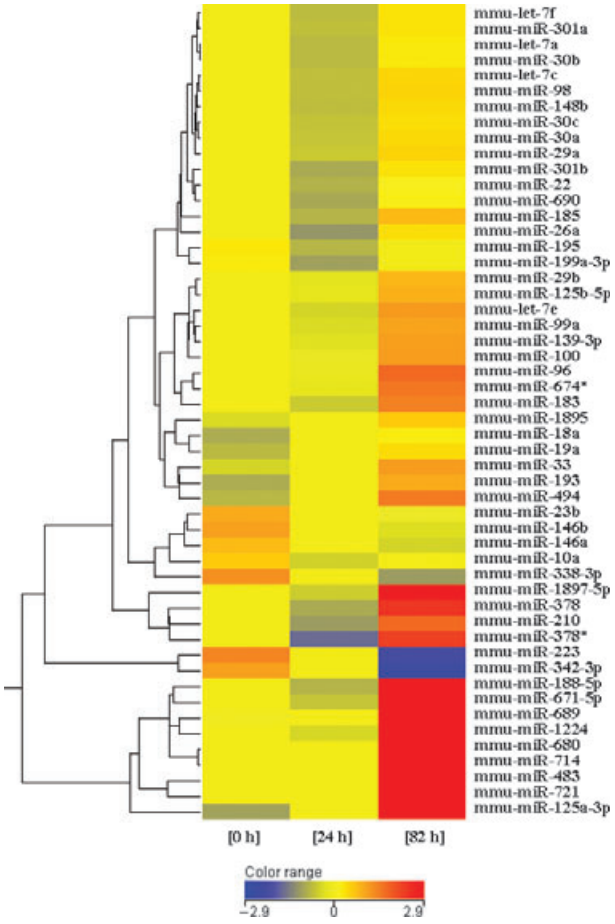

Fig. 5. MicroRNA (miRNA) expression profiles in RANKL-stimulated RAW264.7 cells. The heat map shows the results of a hierarchical cluster analysis of miRNA microarray data (fold change > 2) from RAW264.7 cells stimulated with RANKL (50 ng/mL) for 0, 24 or 82 h. Red, upregulation; blue, downregulation; yellow, median of the three points (0, 24 and 82 h). The miRNAs for which the signal intensities at 0, 24 and 82 h were all weak (< 20) were excluded from the map. This experiment was performed once.

time-dependent downregulation in expression of miR-23b, miR-146a, miR-146b, miR-223 and miR-342-3p, whereas the expression of miR-125a-3p, miR-483, miR-680, miR-689, miR-714 and miR-721 was upregulated in a time-dependent manner. The expression levels of miR-26a, miR-29b, miR-199a-3p, miR-210, miR-378, miR-671-5p and miR-1224 were decreased at 24 h and increased at 82 h after RANKL treatment. Microarray analyses are summarized in Table 1.

qRT-PCR analysis to validate microarray miRNA expression data in RANKL-treated RAW264.7 cells

To validate the microarray data, the levels of representative miRNAs were analyzed by qRT-PCR. Figure 6 shows the relative expression levels of representative miRNAs in RAW264.7 cells treated with RANKL alone. The expression of miR-210 showed RANKL-stimulated upregulation (Fig. 6A), and miR-378 expression was increased 4.8-fold (Fig. 6B). Similarly, miR-1224 expression was upregulated (Fig. 6C). The expression levels of miR-223 and miR-342-3p decreased by more than 20-fold and sixfold, respectively, in a time-dependent manner (Fig. 6D, E). The expression of miR-155 is reportedly downregulated in osteoclasts (25, 26, 28). However, in our study, miR-155 expression did not change significantly in RANKL-treated RAW264.7 cells (Fig. 6F), although it decreased to 0.65-fold in RANKL/M-CSF-treated BMMs (Figure S2F). The expression of miR-21 did not increase significantly in RAW264.7 cells (Fig. 6G) or in BMMs (Figure S2G) after RANKL treatment. Figure S2 shows the validation of these miRNA expression levels in RANKL/M-CSF-treated BMMs. The expression of miR-378 showed a marked 21-fold increase (Figure S2B).

In summary, with the exception of miR-342-3p, the changes in miRNA expression, as determined by qRT-PCR and microarray analyses, were similar between RANKL-treated RAW264.7 cells and RANKL/M-CSF-treated BMMs.

Expression levels of miR-21, miR-29b, miR-146a, miR-155 and miR-210 were higher in TNF-α/RANKL-treated cells compared with RANKL-treated cells

To determine which miRNAs are important in TNF-α-regulated osteoclast differentiation, we compared the results of the microarray analyses of TNF-α/RANKL-treated and RANKL -treated cells. Differences in the expression levels of miR-29b, miR-139-3p, miR-142-3p, miR-142-5p and miR-210 were seen between TNF-α/RANKL-treated and RANKL-treated cells. miR-29b and miR-210 were more highly expressed in TNF-α/RANKL/(M-CSF)-treated cells compared with RANKL/(M-CSF)-treated cells during osteoclast differentiation (Fig. 7C, D, I, and J). As the baseline expression of miR-139-3p was relatively low, no clear correlation was observed between microarray and qRT-PCR data (data not shown). Upregulated expression levels of miR-142-3p and miR-142-5p were observed in TNF-α/RANKL-treated RAW264.7 cells compared with RANKL-treated RAW264.7 cells, but their expression was decreased in BMMs during osteoclast formation (data not shown). Considering the results of the qRT-PCR analyses (Figs 4 and 6; Figures S1 and S2), miR-21 and miR-155 were more highly expressed in TNF-α/RANKL/(M-CSF)-treated cells compared

Table 1. MicroRNAs that were altered by more than twofold in microarray analyses during osteoclast differentiation

	TNF-α/RANKL	RANKL	TNF-α/RANKL RANKL
Downregulation	–	miR-23b, miR-146a, miR-146b, miR-338-3p	miR-223, miR-342-3p
Upregulation	miR-29a, miR-29b, miR-29c, miR-30b, miR-30e, miR-34a, miR-101a, miR-101b, miR-142-3p, miR-142-5p, miR-148b, miR-199a-3p, miR-365, miR-1892, miR-1904	miR-18a, miR-99a, miR-100, miR-378*, miR-714	let-7e, miR-19a, miR-33, miR-96, miR-125a-3p, miR139-3p, miR -183, miR-188-5p, miR-193, miR-210, miR-378, miR-483, miR-494, miR-671-5p, miR-674*, miR-680, miR-689, miR-721, miR-1224, miR-1895, miR-1897-5p

More than twofold indicates tumor necrosis factor alpha (TNF-α)/RANKL treatment (0 vs. 82 h) or RANKL treatment (0 vs. 82 h) or both TNF-α/RANKL treatment (0 vs. 82 h) and RANKL treatment (0 vs. 82 h); fold change > 2.

with RANKL/(M-CSF)-treated cells (Fig. 7A, B, G, and H). Mature miR-146a has been shown to be highly expressed in human gingiva during periodontitis (22) and in the periodontium of ApoE-deficient mice in a murine model of atherosclerosis and experimental periodontitis (23). Although miR-146a expression did not differ by more than twofold between untreated and TNF-α-/RANKL-treated cells in our microarray experiments, it showed higher expression in TNF-α/RANKL/(M-CSF)-treated cells than in RANKL/(M-CSF)-treated cells by qRT-PCR analyses (Fig. 7E, F).

Table 2 shows a list of the miRNAs that were upregulated by more than twofold with TNF-α/RANKL treatment (0 h vs. 24 h, and/or 24 h vs. 82 h, and/or 0 h vs. 82 h) and were highly expressed in periodontitis gingiva compared with healthy gingiva. Perri *et al*. (20) performed PCR array analyses using biopsy samples, gingival epithelium and underlying connective tissue. Lee *et al*. (21) performed PCR array analyses using gingival tissue. Xie *et al*. (22) performed microarray and qRT-PCR analyses using gingival tissue. Of the miRNAs upregulated following TNF-α/RANKL treatment, 17 were also upregulated in periodontitis gingiva compared with healthy gingiva.

Discussion

Our studies examined for the first time global miRNA expression during TNF-α-regulated osteoclast differentiation. Microarray analysis showed that the expression of 44 mature miRNAs differed by more than twofold between untreated cells and cells treated with a combination of TNF-α and RANKL.

The expression of miR-155 in BMMs was upregulated with TNF-α/RANKL/M-CSF treatment, but was downregulated with RANKL/M-CSF treatment (Figures S1 and S2). The upregulation of miR-155 expression has been reported in murine macrophages treated with TNF-α (33), and Mann *et al*. (28) found that miR-155 expression was decreased during osteoclastogenesis. Our findings in BMMs are compatible with these reports. However, our qRT-PCR analysis of miR-155 expression in TNF-α/RANKL-treated RAW264.7 cells revealed transient upregulation (1.5-fold), followed by decreased expression (0.8-fold) (Fig. 4F). Furthermore, there was no significant difference in miR-155 expression between untreated and RANKL-treated RAW264.7 cells (Fig. 6F). It has been reported that fewer osteoclasts are generated *in vitro* from BMMs of miR-155-deficient mice compared with wild-type mice (35). Taken together, these results suggest that miR-155 is upregulated by TNF-α treatment in macrophages, but downregulation of miR-155 may not be necessary for osteoclastogenesis.

In the present study, the expression of miR-146a increased during TNF-α-regulated osteoclast differentiation. miR-146a is NF-κB-dependent and plays an important role in innate immunity by regulating cytokine production (34, 36). Mature miR-146a is highly expressed in human periodontitis gingiva (22) and in experimental periodontitis periodontium (23) in ApoE-deficient mice, the murine model for atherosclerosis. In addition, lipopolysaccharide, a contributing factor in the pathogenesis of periodontal disease, is the most potent stimulator of miR-146a (34). However, miR-146a overexpression inhibits osteoclast formation (37). TNF receptor-associated factor 6, which is an adaptor protein of RANK, is a target gene of hsa-miR-146a (36) and a putative target of mmu-miR-146a, based on TargetScan algorithms (http://www.targetscan.org/). Considering our results and these reports, miR-146a induced by TNF-α/RANKL treatment may serve as a negative feedback regulator of osteoclastogenesis.

TNF-α/RANKL treatment increased miR-21 expression by three- to 4.5-fold compared with expression in untreated RAW264.7 cells and BMMs, and miR-21 is highly expressed in periodontitis gingiva (21). miR-21 is an NF-κB transactivational gene, and depletion of the NF-κB p65 subunit abolished lipopolysaccharide-induced expression of miR-21 (34). Sugatani *et al*.(24) observed upregulation of miR-21, which downregulates the expression of programmed cell death 4, a negative regulator of osteoclastogenesis. However, in the present study, miR-21 expression did not increase as a result of RANKL treatment in RAW264.7 cells or in BMMs. Thus, TNF-α signaling, rather than RANKL signaling, may induce miR-21 expression in osteoclastogenesis.

We observed that TNF-α/RANKL and RANKL treatment triggered the

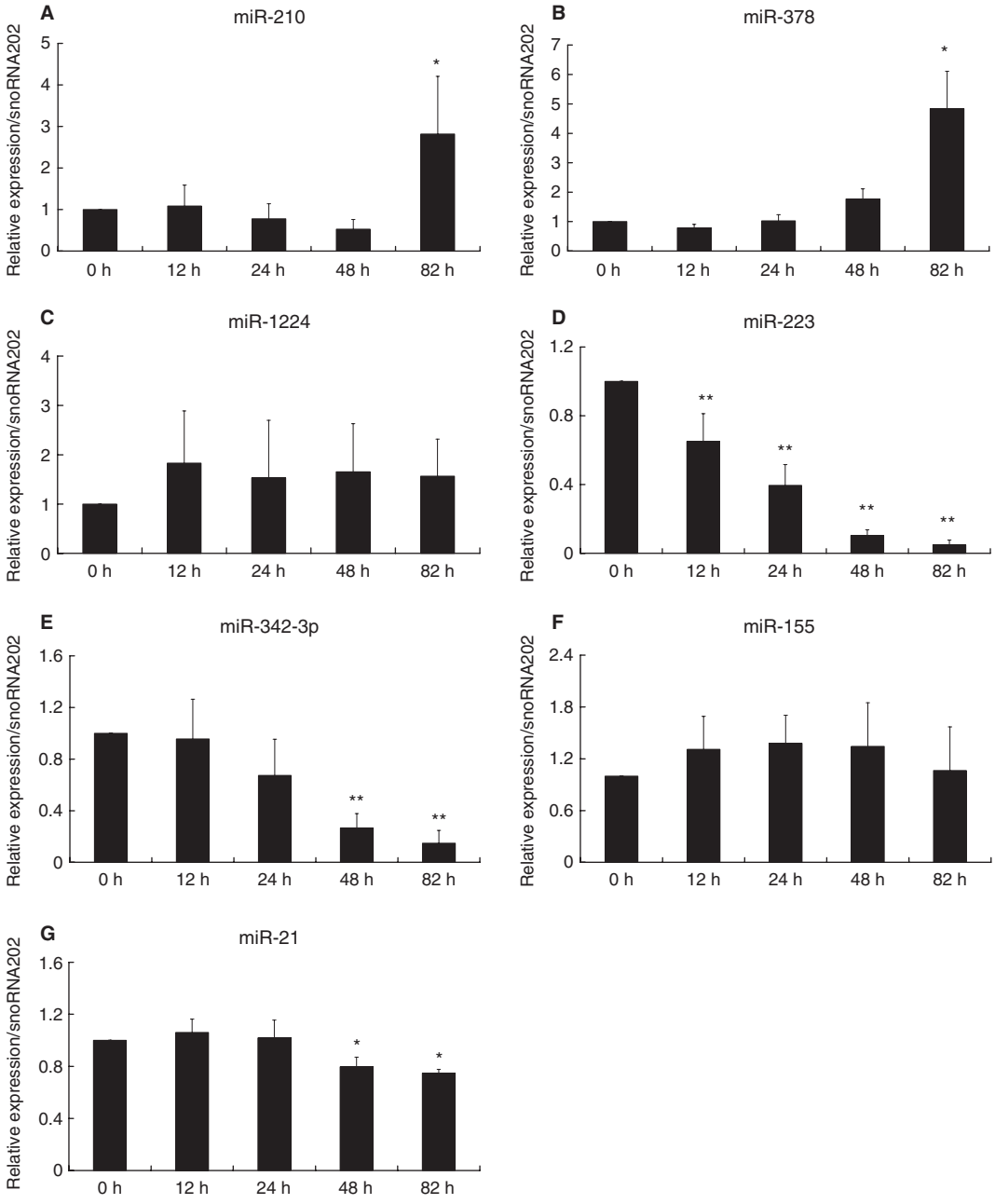

Fig. 6. Quantitative RT-PCR (qRT-PCR) validation of microRNA (miRNA) microarray data in RANKL-treated RAW264.7 cells. RNA isolated from RAW264.7 cells that were cultured in the presence of RANKL (50 ng/mL) for 0, 12, 24, 48 and 82 h were analyzed using qRT-PCR. The expression levels of miR-210 (A), miR-378 (B), miR-1224 (C), miR-223 (D), miR-342-3p (E), miR-155 (F) and miR-21 (G) are shown. Values are relative to 1 at 0 h (before stimulation) for each miRNA. Quantification was performed using snoRNA 202 as an endogenous control. The experiments were performed independently three times. Data are expressed as mean ± standard deviation. One-way analysis of variance was performed. *, $p < 0.05$ vs. 0 h. **, $p < 0.01$ vs. 0 h.

time-dependent downregulation of two miRNAs – miR-223 and miR-342-3p – in RAW264.7 cells. miR-223 regulates *Nfia* and the expression of M-CSF receptor, which is critical for osteoclast differentiation and function (1, 29). It is expressed specifically in mouse $CD11b^+$ myeloid cell lineages, and in human monocytes, granulocytes and platelets (29, 38). The overexpression of miR-223 blocks osteoclast differentiation, whereas the inhibition of miR-223 expression has the reverse effect (29). Although miR-342-3p decreased in RAW264.7 cells during osteoclast formation, it did not decrease in BMMs. This suggests that the downregulation of miR-342-3p may not be essential for osteoclastogenesis.

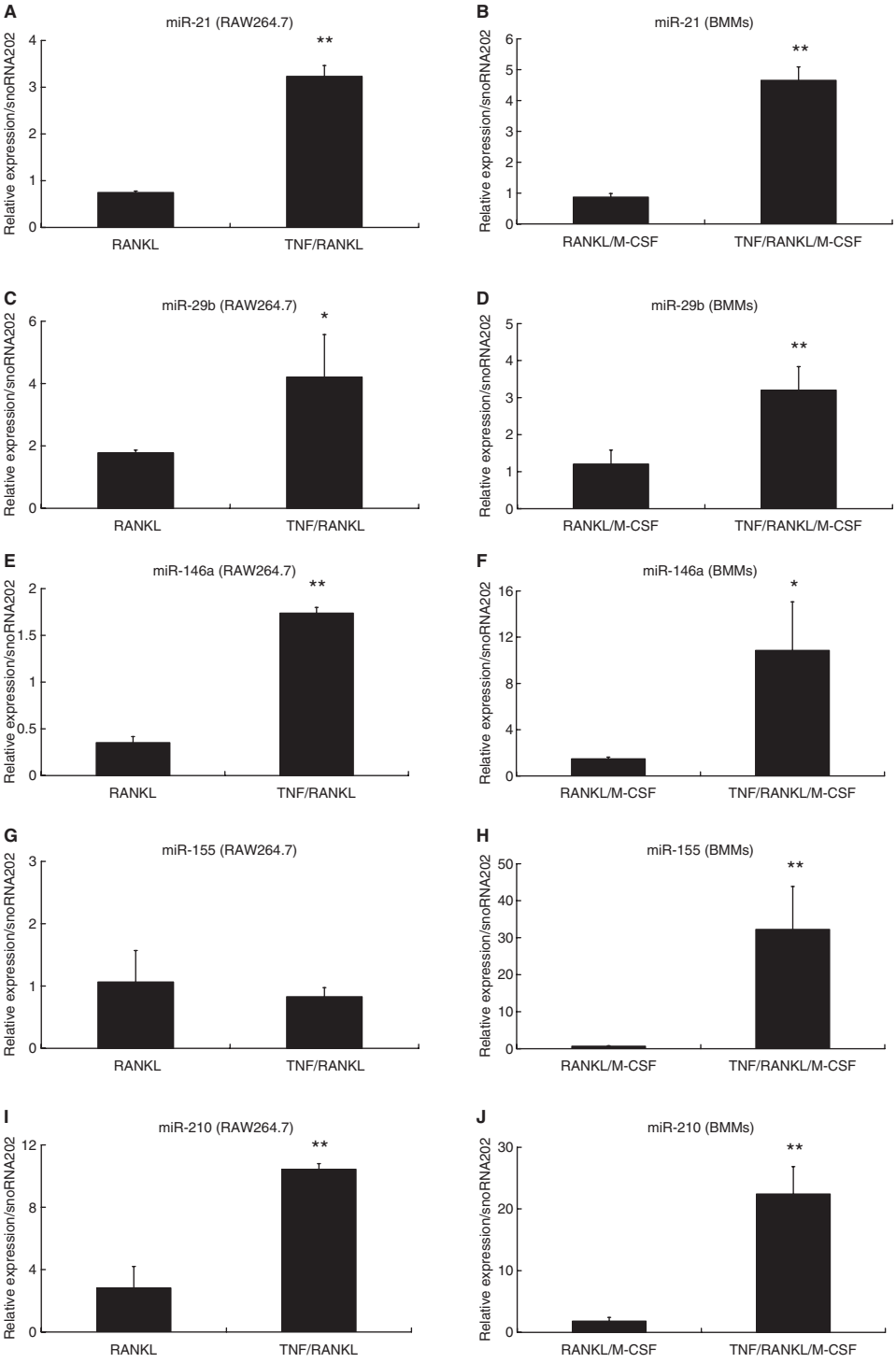

Fig. 7. MicroRNAs (miRNAs) that were highly expressed in tumor necrosis factor alpha (TNF-α)/RANKL-treated cells as compared with RANKL-treated cells. RNA isolated from RAW264.7 cells that were treated with RANKL (50 ng/mL) or TNF-α (50 ng/mL)/RANKL (10 ng/mL) for 82 h was analyzed using quantitative RT-PCR (qRT-PCR). The expression levels of miR-21(A), miR-29b (C), miR-146a (E), miR-155 (G) and miR-210 (I) are shown. Similarly, RNA isolated from bone marrow macrophages (BMMs) that were treated with RANKL (100 ng/mL)/macrophage colony-stimulating factor (M-CSF) (10 ng/mL) or TNF-α (50 ng/mL)/RANKL(20 ng/mL)/M-CSF (10 ng/mL) for 82 h was analyzed using qRT-PCR. The expression levels of miR-21(B), miR-29b (D), miR-146a (F), miR-155 (H) and miR-210 (J) are shown; values are relative to 1 at 0 h (before stimulation) for each miRNA. Quantification was performed using snoRNA 202 as an endogenous control. The experiments were performed independently three times. Data are expressed as mean ± standard deviation. Unpaired two-tailed Student's *t*-tests were performed, assuming unequal variance, to identify significant differences. *, $p < 0.05$ vs. RANKL or RANKL/M-CSF. **, $p < 0.01$ vs. RANKL or RANKL/M-CSF.

Table 2. MicroRNAs (miRNAs) that were upregulated by more than twofold with tumor necrosis factor alpha (TNF-α)/RANKL treatment during osteoclast differentiation and highly expressed miRNAs in the gingiva during periodontitis

miRNA	Reference(s)
let-7e	(21)
miR-18a	(20)
miR-19a	(21, 22)
miR-19b	(21)
miR-21	(21)
miR-22	(20)
miR-29a	(21)
miR-29b	(21)
miR-29c	(21)
miR-30b	(21, 22)
miR-30e	(20–22)
miR-33	(22)
miR-34a	(21)
miR-101a	(21, 22)
miR-142-3p	(20, 22)
miR-146a	(22)
miR-210	(20)

mmu-miR-33 corresponds to hsa-miR-33a. mmu-miR-101a corresponds to hsa-miR-101.

Perri *et al.* performed PCR array analyses using biopsy samples, gingival epithelium, and underlying connective tissue (20). Lee *et al.* performed PCR array analyses using gingival tissue (21). Xie *et al.* performed microarray and qRT-PCR analyses using gingival tissue (22). More than two-fold indicates TNF-α/RANKL treatment (0 vs. 24 h, and/or 24 vs. 82 h, and/or 0 vs. 82 h) in microarray analysis and/or qRT-PCR analyses; fold change > 2.

In the present study, miR-29b and miR-210 were upregulated in cells treated with TNF-α/RANKL compared with the levels in RANKL-treated cells. Both miR-29b and miR-210 are increased in the gingiva during periodontitis (20–22). The expression of miR-29b is induced by NF-κB in leukemia (34). miR-210 regulates various genes involved in the cell cycle, differentiation, development, membrane trafficking and migration/adhesion (39, 40).

We also observed that miR-1224 expression increased during TNF-α-regulated osteoclast differentiation in RAW 264.7 cells. Transfection with miR-1224 mimics reportedly reduces TNF-α promoter activity in RAW264.7 cells, and the inhibition of miR-1224 increases TNF-α promoter activity (41). miR-1224 negatively affects the transcription of TNF-α mRNA by targeting specificity protein 1, which controls TNF-α expression (41). The present study suggests that upregulation of miR-1224 during TNF-α-stimulated osteoclast differentiation may have a negative feedback effect in TNF-α-treated RAW264.7 cells.

The present study demonstrated that miR-378 expression increased during osteoclast differentiation in both RAW264.7 cells and BMMs, exhibiting a 21-fold increase in RANKL/M-CSF-treated BMMs. We originally hypothesized that knockdown of miR-378 would inhibit osteoclastogenesis and that overexpression of miR-378 would promote it. Unexpectedly, both knockdown and overexpression of miR-378 inhibited osteoclast formation (Tadayoshi Kagiya personal observation). miR-378 promotes cell survival and participates in blood vessel formation (42). miR-378 binds to the 3′ untranslated region of caspase-3 mRNA and inhibits the expression of caspase-3 and apoptosis in rat cardiac myocytes (43). In contrast, active caspase-3 is required for osteoclast differentiation (44). The number of osteoclasts in the long bones of procaspase-3 knockout mice was decreased compared with wild-type mice (44). Overexpression of miR-378 may inhibit both caspase-3 expression and osteoclast differentiation. Our findings, and reports by others, indicate that miR-378 upregulation in osteoclasts is crucial for their differentiation; however, an excess of miR-378 suppresses osteoclast formation.

$CD11b^{+}$-cre/dicer null mice have mild osteopetrosis caused by decreased osteoclast numbers and bone resorption (1). Mizoguchi *et al.* (45) reported that cathepsin k-cre/dicer null mice have increased bone mass caused by decreased osteoclast numbers and bone resorption. However, they did not observe remarkable upregulation of miRNA expression in miRNA microarray analyses of murine bone marrow cells 24 h post-RANKL stimulation. In the present study, at 24 h post-TNF-α/RANKL treatment, only 12 mature miRNAs were upregulated by more than twofold in RAW264.7 cells. In contrast, at 82 h post-treatment, 42 miRNAs, including miR-378, were upregulated by more than twofold. This suggests that multiple miRNAs suppress the expression of many target genes during the late stages of osteoclast differentiation.

In the present study, we used both a murine cell line and bone marrow cells. miRNAs are widely known to repress gene expression through sequence-specific base pairing with binding sites in the 3′ untranslated regions of target transcripts (1, 17–19), and murine and human binding sites are often conserved. However, it is necessary to validate our results in human osteoclasts in future studies. Recent studies have shown that miRNAs can repress mRNAs by binding to other sites in target genes (46, 47). Li *et al.* (46) demonstrated that miR-2861 targets the CDS region of HDAC5, and Tay *et al.* (47) revealed that miR-134, miR-296 and miR-470 target the CDS regions of transcription factors. These reports and our results indicate that multiple miRNA target genes must exist during osteoclast differentiation.

Here, we demonstrated that the combination of TNF-α and RANKL regulates the expression of many mature miRNAs during osteoclast formation. More than one-third of the miRNAs upregulated during TNF-α/RANKL-regulated osteoclastogenesis are highly expressed in the gingiva during periodontitis. miRNAs may be transported to and from osteoclasts if they exist in exosomes, which are released into the extracellular environment and function in the intercellular transport of miRNAs (18, 26, 48, 49). In the future, miRNA therapy may be useful for treating periodontal disease. Although a single miRNA generally represses the production of hundreds of proteins, the repression is typically mild (50). Considering this mild effect, it may be necessary to combine miRNA-based and traditional routine therapies to successfully treat periodontal disease.

Acknowledgements

We are especially thankful to Professor Emeritus Teruo Tanaka, Kyushu University, for his kind advice and expertise. We also thank Dr Takayoshi Yamaza, Kyushu University Graduate School of Dental Science, for his advice on our research. In addition, we thank Professor Hidemitsu Harada, Professor Emeritus Tokio Nawa, Professor Hiroyuki Miura, Professor Akira Fujimura and Dr Yoshinori Ando, Iwate Medical University, for reading the manuscript and giving helpful advice. This study was supported, in part, by grants from the Keiryokai Research Foundation (No. 97 to T.K.), a Grant-in-Aid for Young Scientists (B) (No. 21791830 to T.K.), Scientific Research (C) (No. 23593042 to T.K.) and a Grant-in-Aid for Strategic Medical Science Research Center (2010–2014) from the Ministry of Education, Culture, Sports, Science and Technology, Japan.

Conflict of interest

The authors declare no conflict of interest.

Supporting Information

Additional Supporting Information may be found in the online version of this article:

Table S1 Primer pairs used in qRT-PCR analyses.

Table S2 Microarray signal intensities altered by more than twofold by TNF-α/RANKL treatment.

Table S3 Microarray signal intensities altered by more than twofold with RANKL treatment.

Fig. S1 qRT-PCR validation of miRNA microarray data in TNF-α/RANKL/M-CSF-treated BMMs.

Fig. S2 qRT-PCR validation of miRNA microarray data in RANKL/M-CSF-treated BMMs.

Please note: Wiley-Blackwell are not responsible for the content or functionality of any supporting materials supplied by the authors. Any queries (other than missing material) should be directed to the corresponding author for the article.

References

1. Sugatani T, Hruska KA. Impaired micro-RNA pathways diminish osteoclast differentiation and function. *J Biol Chem* 2009;**284**:4667–4678.
2. Boyle WJ, Simonet WS, Lacey DL. Osteoclast differentiation and activation. *Nature* 2003;**423**:337–342.
3. Taubman MA, Valverde P, Han X, Kawai T. Immune response: the key to bone resorption in periodontal disease. *J Periodontol* 2005;**76**:2033–2041.
4. Hosokawa Y, Hosokawa I, Ozaki K, Nakae H, Matsuo T. Cytokines differentially regulate CXCL10 production by interferon-gamma-stimulated or tumor necrosis factor-alpha-stimulated human gingival fibroblasts. *J Periodontal Res* 2009;**44**:225–231.
5. Takeshita S, Kaji K, Kudo A. Identification and characterization of the new osteoclast progenitor with macrophage phenotypes being able to differentiate into mature osteoclasts. *J Bone Miner Res* 2000;**15**:1477–1488.
6. Teitelbaum SL. RANKing c-Jun in osteoclast development. *J Clin Invest* 2004;**114**:463–465.
7. Yogesha SD, Khapli SM, Wani MR. Interleukin-3 and granulocyte-macrophage colony-stimulating factor inhibits tumor necrosis factor (TNF)-alpha-induced osteoclast differentiation by down-regulation of expression of TNF receptors 1 and 2. *J Biol Chem* 2005;**280**:11759–11769.
8. Lam J, Takeshita S, Barker JE, Kanagawa O, Ross FP, Teitelbaum SL. TNF-alpha induces osteoclastogenesis by direct stimulation of macrophages exposed to permissive levels of RANK ligand. *J Clin Invest* 2000;**106**:1481–1488.
9. Wang PL, Ohura K, Fujii T, *et al*. DNA microarray analysis of human gingival fibroblasts from healthy and inflammatory gingival tissues. *Biochem Biophys Res Commun* 2003;**305**:970–973.
10. Kook SH, Jang YS, Lee JC. Human periodontal ligament fibroblasts stimulate osteoclastogenesis in response to compression force through TNF-alpha-mediated activation of CD4+ T cells. *J Cell Biochem* 2011;**112**:2891–2901.
11. Garlet GP, Cardoso CR, Campanelli AP, Martins W Jr, Silva JS. Expression of suppressors of cytokine signaling in diseased periodontal tissues: a stop signal for disease progression? *J Periodontal Res* 2006;**41**:580–584.
12. Gaspersic R, Stiblar-Martincic D, Osredkar J, Skaleric U. In vivo administration of recombinant TNF-alpha promotes bone resorption in mice. *J Periodontal Res* 2003;**38**:446–448.
13. Figueredo CM, Brito F, Barros FC, *et al*. Expression of cytokines in the gingival crevicular fluid and serum from patients with inflammatory bowel disease and untreated chronic periodontitis. *J Periodontal Res* 2011;**46**:141–146.
14. Lu J, Getz G, Miska EA, *et al*. MicroRNA expression profiles classify human cancers. *Nature* 2005;**435**:834–838.
15. Cimmino A, Calin GA, Fabbri M, *et al*. miR-15 and miR-16 induce apoptosis by targeting BCL2. *Proc Natl Acad Sci U S A* 2005; **102**: 13944–13949.
16. Koh TC, Lee YY, Chang SQ, Nissom PM. Identification and expression analysis of miRNAs during batch culture of HEK-293 cells. *J Biotechnol* 2009;**140**:149–155.
17. Li Z, Hassan MQ, Volinia S, *et al*. A microRNA signature for a BMP2-induced osteoblast lineage commitment program. *Proc Natl Acad Sci U S A* 2008;**105**:13906–13911.
18. Kosaka N, Iguchi H, Yoshioka Y, Takeshita F, Matsuki Y, Ochiya T. Secretory mechanisms and intercellular transfer of microRNAs in living cells. *J Biol Chem* 2010;**285**:17442–17452.
19. Guo H, Ingolia NT, Weissman JS, Bartel DP. Mammalian microRNAs predominantly act to decrease target mRNA levels. *Nature* 2010;**466**:835–840.
20. Perri R, Nares S, Zhang S, Barros SP, Offenbacher S. MicroRNA modulation in obesity and periodontitis. *J Dent Res* 2012;**91**:33–38.
21. Lee YH, Na HS, Jeong SY, Jeong SH, Park HR, Chung J. Comparison of inflammatory microRNA expression in healthy and periodontitis tissues. *Biocell* 2011;**35**:43–49.
22. Xie YF, Shu R, Jiang SY, Liu DL, Zhang XL. Comparison of microRNA profiles of human periodontal diseased and healthy gingival tissues. *Int J Oral Sci* 2011;**3**:125–134.
23. Nahid MA, Rivera M, Lucas A, Chan EK, Kesavalu L. Polymicrobial infection with periodontal pathogens specifically enhances microRNA miR-146a in ApoE-/- mice during experimental periodontal disease. *Infect Immun* 2011;**79**:1597–1605.
24. Sugatani T, Vacher J, Hruska KA. A microRNA expression signature of osteoclastogenesis. *Blood* 2011;**117**:3648–3657.
25. Kapinas K, Delany AM. MicroRNA biogenesis and regulation of bone remodeling. *Arthritis Res Ther* 2011;**13**:220.
26. Lian JB, Stein GS, van Wijnen AJ, *et al*. MicroRNA control of bone formation and homeostasis. *Nat Rev Endocrinol* 2012; **8**: 212–227.
27. Xia Z, Chen C, Chen P, Xie H, Luo X. MicroRNAs and their roles in osteoclast differentiation. *Front Med* 2011;**5**:414–419.

28. Mann M, Barad O, Agami R, Geiger B, Hornstein E. miRNA-based mechanism for the commitment of multipotent progenitors to a single cellular fate. *Proc Natl Acad Sci U S A* 2010;**107**:15804–15809.
29. Sugatani T, Hruska KA. MicroRNA-223 is a key factor in osteoclast differentiation. *J Cell Biochem* 2007;**101**:996–999.
30. Dong S, Yang B, Guo H, Kang F. MicroRNAs regulate osteogenesis and chondrogenesis. *Biochem Biophys Res Commun* 2012;**418**:587–591.
31. Bak M, Silahtaroglu A, Moller M, *et al*. MicroRNA expression in the adult mouse central nervous system. *RNA* 2008;**14**:432–444.
32. Lin EA, Kong L, Bai XH, Luan Y, Liu CJ. miR-199a, a bone morphogenic protein 2-responsive MicroRNA, regulates chondrogenesis via direct targeting to Smad1. *J Biol Chem* 2009;**284**:11326–11335.
33. O'Connell RM, Taganov KD, Boldin MP, Cheng G, Baltimore D. MicroRNA-155 is induced during the macrophage inflammatory response. *Proc Natl Acad Sci U S A* 2007;**104**:1604–1609.
34. Ma X, Becker Buscaglia LE, Barker JR, Li Y. MicroRNAs in NF-kappaB signaling. *J Mol Cell Biol* 2011;**3**:159–166.
35. Bluml S, Bonelli M, Niederreiter B, *et al*. Essential role of microRNA-155 in the pathogenesis of autoimmune arthritis in mice. *Arthritis Rheum* 2011;**63**:1281–1288.
36. Taganov KD, Boldin MP, Chang KJ, Baltimore D. NF-kappaB-dependent induction of microRNA miR-146, an inhibitor targeted to signaling proteins of innate immune responses. *Proc Natl Acad Sci U S A* 2006;**103**:12481–12486.
37. Nakasa T, Shibuya H, Nagata Y, Niimoto T, Ochi M. The inhibitory effect of microRNA-146a expression on bone destruction in collagen-induced arthritis. *Arthritis Rheum* 2011;**63**:1582–1590.
38. Merkerova M, Belickova M, Bruchova H. Differential expression of microRNAs in hematopoietic cell lineages. *Eur J Haematol* 2008;**81**:304–310.
39. Fasanaro P, Greco S, Lorenzi M, *et al*. An integrated approach for experimental target identification of hypoxia-induced miR-210. *J Biol Chem* 2009;**284**:35134–35143.
40. Tsuchiya S, Fujiwara T, Sato F, *et al*. MicroRNA-210 regulates cancer cell proliferation through targeting fibroblast growth factor receptor-like 1 (FGFRL1). *J Biol Chem* 2011;**286**:420–428.
41. Niu Y, Mo D, Qin L, *et al*. Lipopolysaccharide-induced miR-1224 negatively regulates tumour necrosis factor-alpha gene expression by modulating Sp1. *Immunology* 2011;**133**:8–20.
42. Lee DY, Deng Z, Wang CH, Yang BB. MicroRNA-378 promotes cell survival, tumor growth, and angiogenesis by targeting SuFu and Fus-1 expression. *Proc Natl Acad Sci U S A* 2007;**104**:20350–20355.
43. Fang J, Song XW, Tian J, *et al*. Overexpression of microRNA-378 attenuates ischemia-induced apoptosis by inhibiting caspase-3 expression in cardiac myocytes. *Apoptosis* 2012;**17**:410–423.
44. Szymczyk KH, Freeman TA, Adams CS, Srinivas V, Steinbeck MJ. Active caspase-3 is required for osteoclast differentiation. *J Cell Physiol* 2006;**209**:836–844.
45. Mizoguchi F, Izu Y, Hayata T, *et al*. Osteoclast-specific Dicer gene deficiency suppresses osteoclastic bone resorption. *J Cell Biochem* 2010;**109**:866–875.
46. Li H, Xie H, Liu W, *et al*. A novel microRNA targeting HDAC5 regulates osteoblast differentiation in mice and contributes to primary osteoporosis in humans. *J Clin Invest* 2009;**119**:3666–3677.
47. Tay Y, Zhang J, Thomson AM, Lim B, Rigoutsos I. MicroRNAs to Nanog, Oct4 and Sox2 coding regions modulate embryonic stem cell differentiation. *Nature* 2008;**455**:1124–1128.
48. Valadi H, Ekstrom K, Bossios A, Sjostrand M, Lee JJ, Lotvall JO. Exosome-mediated transfer of mRNAs and microRNAs is a novel mechanism of genetic exchange between cells. *Nat Cell Biol* 2007;**9**:654–659.
49. Skog J, Wurdinger T, van Rijn S, *et al*. Glioblastoma microvesicles transport RNA and proteins that promote tumour growth and provide diagnostic biomarkers. *Nat Cell Biol* 2008;**10**:1470–1476.
50. Selbach M, Schwanhausser B, Thierfelder N, Fang Z, Khanin R, Rajewsky N. Widespread changes in protein synthesis induced by microRNAs. *Nature* 2008;**455**:58–63.